

**HIPPOCAMPUS SEGMENTATION USING  
LOCALLY INTEGRATED PRIOR-BASED LEVEL  
SET GUIDED BY ASSEMBLED AND WEIGHTED  
COHERENT POINT DRIFT REGISTRATION**

**ANUSHA ACHUTHAN**

**UNIVERSITI SAINS MALAYSIA**

**2016**

**HIPPOCAMPUS SEGMENTATION USING  
LOCALLY INTEGRATED PRIOR-BASED LEVEL  
SET GUIDED BY ASSEMBLED AND WEIGHTED  
COHERENT POINT DRIFT REGISTRATION**

**by**

**ANUSHA ACHUTHAN**

**Thesis submitted in fulfilment of the requirements  
for the degree of  
Doctor of Philosophy**

**March 2016**

# ACKNOWLEDGEMENT

Praises and thanks to the God, the Almighty for showering me with the blessings to pursue this dream successfully. I would not have pen down this thesis without the continuous support from a group of special hearts.

First, and foremost, my deepest gratitude and appreciation goes to my research supervisor, Professor Dr. Mandava Rajeswari for guiding me towards the path of success. Her passionate guidance has showed me how a true researcher should be. I value most your insights and thoughtful advices during my journey towards PHD.

To my co-supervisor, Dr. Salmah Jalaluddin for her assistance in enhancing my medical knowledge. My special thanks also goes to the field experts, Dr. Dimitrios Zarpalas (Information Technologies Institute, Greece) and Dr. Ou Yangming (Harvard Medical School) for timely facilitation in strengthening my understanding in medical image processing.

My appreciation also goes to my fellow research mates, Rahma, Adilah, Mogana, and Lim Khai Yin for accompanying this research journey with good support.

There are not enough words to describe the encouragement from my lovely parents, Achuthan and Vasunthathevi. Without your love and blessings, I would not stand high as I am today. To my siblings, Abhilashini and Aghilesh, thank you for always being there.

Finally, in fact the most precious ones in my life. My loves and thanks to my hubby, Satrishson for his continuous love and support during this time frame. Without him, I would not have accomplish this height of achievement. And also to my daughter, Tusharaa, the jewel of my life, which brightens my arduous days with her cheekiness.

# TABLE OF CONTENTS

	<b>Page</b>
<b>ACKNOWLEDGEMENT</b> .....	ii
<b>TABLE OF CONTENTS</b> .....	iii
<b>LIST OF TABLES</b> .....	viii
<b>LIST OF FIGURES</b> .....	ix
<b>LIST OF ABBREVIATIONS</b> .....	xiii
<b>ABSTRAK</b> .....	xv
<b>ABSTRACT</b> .....	xviii
 <b>CHAPTER 1 – INTRODUCTION</b>	
1.1 Medical Image Segmentation .....	1
1.2 Trends in Medical Image Segmentation .....	2
1.3 Hippocampus .....	5
1.4 Problem Statement .....	7
1.5 Objectives .....	12
1.6 Scope .....	12
1.7 Significance of the Study .....	13
1.8 Overview of Methodology .....	13
1.9 Contributions .....	14
1.10 Organization of the Thesis .....	15
 <b>CHAPTER 2 – BACKGROUND</b>	
2.1 Magnetic Resonance Imaging .....	17
2.1.1 Imaging Characteristics .....	18
2.1.2 Imaging Coordinates and Planes .....	18
2.1.3 Brain Magnetic Resonance Imaging .....	20

2.2	Medical Image Registration .....	21
2.2.1	Type of Transformation .....	22
2.2.2	Nature of Registration Algorithms .....	23
2.3	Deformable Models .....	24
2.3.1	Parametric Models .....	24
2.3.2	Level Set .....	26
2.3.2(a)	Edge-based Level Set .....	29
2.3.2(b)	Region-based Level Set .....	31
2.3.2(c)	Hybrid Level Set .....	32

### **CHAPTER 3 – RELATED WORK**

3.1	Brain Structure Segmentation Approaches .....	34
3.1.1	Manual or Semi-automatic .....	36
3.1.2	Fuzzy Spatial Relation-based .....	37
3.1.3	Atlas-based .....	39
3.1.3(a)	Issues in atlas-based segmentation approaches .....	44
3.1.3(b)	Extension to atlas-based segmentation approaches .....	45
3.1.4	Statistical Shape Model-based .....	46
3.1.4(a)	Phase 1: SSM Construction .....	48
3.1.4(b)	Phase 2: Segmentation .....	52
3.2	Prior-based Level Set Segmentation .....	54
3.3	Conclusion and Direction .....	57

### **CHAPTER 4 – HIPPOCAMPUS SEGMENTATION: METHODOLOGY**

4.1	Hippocampus Segmentation: Methodology .....	63
4.2	Datasets .....	64
4.2.1	Dataset 1: OASIS-MICCAI .....	65

4.2.2	Dataset 2: IBSR .....	67
4.3	Experimental Setup .....	69
4.4	Evaluation Criteria .....	69
4.4.1	Root Mean Square Error .....	70
4.4.2	Dice Similarity Coefficient .....	70
4.4.3	False Positive .....	70
4.4.4	Visual Comparisons .....	71
4.5	Summary .....	71
 <b>CHAPTER 5 – PHASE I: PRIOR MODEL CONSTRUCTION</b>		
5.1	Related Point Set Registration Methods .....	72
5.2	The Proposed Prior Model Construction Approach.....	74
5.2.1	Non-rigid Registration .....	75
5.2.2	Label Propagation .....	77
5.2.3	Generation of Point Set .....	77
5.2.4	Assembled and Weighted CPD .....	78
5.3	The Algorithm for Prior Model Construction .....	84
5.4	Computational Complexity of AWCPD .....	85
5.5	Experimental Results .....	87
5.5.1	Experiment 1: Parameters setting of AWCPD.....	87
5.5.2	Experiment 2: Evaluation of AWCPD .....	89
5.5.3	Experiment 3: Comparison with other prior model construction approaches .....	91
5.5.3(a)	Quantitative Measure .....	92
5.5.3(b)	3D Visual Comparisons .....	96
5.5.3(c)	Conclusion.....	101

## **CHAPTER 6 – PHASE II: HIPPOCAMPUS SEGMENTATION**

6.1	Analysis of Hippocampus Characteristics .....	103
6.2	Proposed Hippocampus Segmentation Approach .....	106
6.2.1	Prior Mask Construction .....	106
6.2.2	3D Edge Detection .....	108
6.2.3	Prior Mask Refinement .....	110
6.2.4	Locally Integrated Prior-based Level Set .....	110
6.2.4(a)	GAC Term : $E(\phi_{GAC})$ .....	112
6.2.4(b)	Prior Term : $E(\phi_P)$ .....	112
6.2.4(c)	Complete Energy Function : $E(\phi)$ .....	113
6.2.5	Implementation Details of Locally Integrated Prior-based Level Set .....	114
6.2.5(a)	Initialization for Level Set, $\phi_{t=0}$ .....	114
6.2.5(b)	Surface Movement .....	116
6.3	Experimental Results .....	116
6.3.1	Experiment 1: Performance of Locally Integrated Prior-based Level Set .....	116
6.3.2	Experiment 2: Comparison with state-of-the-art hippocampus segmentation approaches .....	124

## **CHAPTER 7 – CONCLUSION AND FUTURE WORK**

7.1	Conclusion .....	126
7.2	Limitations .....	127
7.3	Future Directions .....	128

<b>REFERENCES</b> .....	130
-------------------------	-----

<b>APPENDICES</b> .....	143
-------------------------	-----

<b>APPENDIX A – IMAGE PROCESSING FUNCTIONS/TOOLS .....</b>	<b>144</b>
A.1 Brain Extraction Tool .....	144
A.2 Advanced Normalization Tools .....	146
A.3 Function Isosurface in Matlab .....	148
A.4 Crust Triangulation .....	148
A.5 Voxelization.....	149
A.6 Fuzzy C-Means Clustering .....	149
A.7 Morphological Operation .....	150
A.7.1 Erosion.....	151
A.7.2 Dilation .....	152
<b>APPENDIX B – ADDITIONAL EXPERIMENTAL RESULTS.....</b>	<b>153</b>
B.1 Segmentation Results of OASIS-MICCAI Dataset .....	153
<b>LIST OF PUBLICATIONS .....</b>	<b>155</b>



## LIST OF TABLES

		<b>Page</b>
Table 3.1	Summary of key literature on brain structures segmentation	61
Table 3.2	Summary of key literature on brain structures segmentation	62
Table 4.1	Details of training (T#) and testing (S#) brain MR volumes in OASIS-MICCAI	66
Table 4.2	Details of IBSR dataset	68
Table 5.1	Comparison of average RMSE values (voxels) of 20 test data using the AWCPD_W1, AWCPD_W2 and ACPD approaches.	90
Table 6.1	Comparison of average Dice similarity coefficient values for hippocampus segmentation approaches using average Dice, and its corresponding standard deviations values (if available) for the IBSR dataset.	125

# LIST OF FIGURES

		Page
Figure 1.1	Information utilized by medical experts in performing manual delineation.	2
Figure 1.2	The different eras of medical image segmentation.	3
Figure 1.3	(a) Anatomy of the brain, relating to the location of temporal lobe ( <i>Serendip Studio</i> , 2015). (b) The location of hippocampus in the brain ( <i>Human Illnesses and Behavioral Health</i> , 2015).	6
Figure 1.4	Overview of the hippocampus structure ( <i>IcoMetrix</i> , 2015).	6
Figure 1.5	Hippocampus being highlighted in green (right hippocampus) and red (left hippocampus) in (a) axial, (b) coronal, and (c) sagittal views, respectively.	7
Figure 1.6	An example of a brain MR image in the coronal view, highlighting the hippocampus and the amygdala.	8
Figure 1.7	(a) A sample of synthetic image. (b) Edge gradient magnitude of the synthetic image with the weak or missing edges highlighted.	12
Figure 2.1	The imaging coordinates and planes in MRI ( <i>3D Slicer</i> , 2015).	19
Figure 2.2	Comparison between (a) T1-weighted and (b) T2-weighted brain MR images ( <i>BRATS: Multimodal Brain Tumor Segmentation Challenge</i> , 2015).	21
Figure 2.3	Level set function with evolving contour $C$ embedded as zero level set (in black).	27
Figure 3.1	Taxonomy of Brain Structure Segmentation Approaches.	35
Figure 3.2	Fuzzy map representing spatial relations between lateral ventricle (LV) and caudate nucleus (Cd), with values ranging from 0 (black) to 1 (white). (a) Original image. (b) Fuzzy map representing a single spatial relation of <i>caudate neclues is near to the lateral ventricle</i> (Colliot et al., 2006). (c) Fuzzy map obtained from fusion of few spatial relations (Bloch et al., 2005).	39
Figure 3.3	Overview of atlas-based segmentation approach.	41
Figure 3.4	Sample images depicting issues of hole and outlier issues using locally weighted and statistical fusions (Landman et al., 2012).	45

Figure 3.5	Overview of Statistical Shape Model-based segmentation.	47
Figure 4.1	The two main phases of the proposed hippocampus segmentation.	64
Figure 4.2	Examples of brain MR images in OASIS-MICCAI dataset in (a) axial, (b) coronal, and (c) sagittal views, viewed using MIPAV software (McAuliffe et al., 2001).	67
Figure 4.3	Examples of IBSR data in (a) axial, (b) coronal, and (c) sagittal views, viewed using MIPAV software (McAuliffe et al., 2001).	69
Figure 5.1	Overview of proposed prior model construction approach.	76
Figure 5.2	(a) Surface triangulation of a labeled image. (b) Point set representation.	78
Figure 5.3	An example of assembled training point sets.	83
Figure 5.4	The core components of (a) AWCPD and (b) GCPD.	87
Figure 5.5	The average RMSE values corresponding to varying values of $\lambda$ .	89
Figure 5.6	Comparison of RMSE values for every test subject using AWCPD, Joint Label Fusion and Mean Shape in SDM.	93
Figure 5.7	The left hippocampus of Subject 3 (blue), with the training dataset (red).	94
Figure 5.8	The right hippocampus of Subject 8 (blue), with the training dataset (red).	95
Figure 5.9	Boxplots illustrating the RMSE values of the AWCPD, Joint Label Fusion and Mean Shape in SDM.	96
Figure 5.10	3D visual comparisons of the constructed prior model of hippocampus with best case from the AWCPD, Joint Label Fusion and Mean Shape in SDM for four different views.	99
Figure 5.11	3D visual comparisons of the constructed prior model of hippocampus with worst case from the AWCPD, Joint Label Fusion and Mean Shape in SDM for four different views.	100
Figure 6.1	Edge gradient magnitude of two samples of 2D coronal slices. The white arrow denotes fragments with missing edges, and red arrow denotes strong edges.	105
Figure 6.2	Block diagram of the proposed hippocampus segmentation approach.	107

Figure 6.3	(a) 3D point set. (b) 3D triangulation of the point set in (a) using Crust algorithm.	108
Figure 6.4	The process of obtaining the edge gradient magnitude inside a volume of interest of the hippocampus $g(I_{VOI})$ using a sample coronal slice.	109
Figure 6.5	The process of obtaining the refined prior mask $PM_R$ using a sample coronal slice.	111
Figure 6.6	Computation of initialization for LocPLS.	115
Figure 6.7	The initialization mask (red), with outline of the ground truth (blue) on sample coronal slices of three subjects from the OASIS-MICCAI dataset.	118
Figure 6.8	Boxplots showing the segmentation accuracy, in terms of Dice similarity coefficients for LocPLS, GPLS and GAC.	120
Figure 6.9	Boxplots showing the RMSE values for LocPLS, GPLS and GAC.	120
Figure 6.10	Boxplots showing the False Positive rates of LocPLS, GPLS and GAC.	121
Figure 6.11	The best segmentation case from OASIS-MICCAI dataset (Subject ID#1). The resulted 3D segmentation (purple) of LocPLS, GPLS and GAC methods, with the corresponding 3D reconstruction of True Positive (blue), False Positive (green), and False Negative (pink). A sample sagittal slice outlining the segmented result (pink) and the ground truth (yellow).	122
Figure 6.12	The worst segmentation case from OASIS-MICCAI dataset (Subject ID#8). The resulted 3D segmentation (purple) of LocPLS, GPLS and GAC methods, with the corresponding 3D reconstruction of True Positive (blue), False Positive (green), and False Negative (pink). A sample sagittal slice outlining the segmented result (pink) and the ground truth (yellow).	123
Figure A.1	Accessing BET from the FSL graphical user interface.	145
Figure A.2	GUI of Brain Extraction Tool.	145
Figure A.3	Erosion of an image, $A$ using structuring element, $B$ with the resultant eroded image, $A \ominus B$ .	151
Figure A.4	Dilation of an image, $A$ using structuring element, $B$ with the resultant dilated image, $A \oplus B$ .	152

Figure B.1      The corresponding 3D reconstruction of True Positive(blue), False Positive (green), and False Negative (pink) for sample subjects from the OASIS-MICCAI dataset.

154

## LIST OF ABBREVIATIONS

<b>2D</b>	2 Dimensional
<b>3D</b>	3 Dimensional
<b>AAM</b>	Active Appearance Model
<b>ANTs</b>	Advanced Normalization Tools
<b>ASM</b>	Active Shape Model
<b>AWCPD</b>	Assembled and Weighted Coherent Point Drift
<b>BET</b>	Brain Extraction Tool
<b>CPD</b>	Coherent Point Drift
<b>DSC</b>	Dice Similarity Coefficient
<b>EM</b>	Expectation-Maximization
<b>EM-ICP</b>	Expectation-Maximization-Iterative Closest Point
<b>GAC</b>	Geodesic Active Contour
<b>GMM</b>	Gaussian Mixture Model
<b>GPLS</b>	Globally Integrated Prior-based Level Set
<b>GVF</b>	Gradient Vector Flow
<b>IBSR</b>	Internet Brain Segmentation Repository
<b>LocPLS</b>	Locally Integrated Prior-based Level Set

<b>MIPAV</b>	Medical Image Processing, Analysis and Visualization
<b>MR</b>	Magnetic Resonance
<b>MRI</b>	Magnetic Resonance Imaging
<b>NIFTI</b>	Neuroimaging Informatics Technology Initiative
<b>NMR</b>	Nuclear Magnetic Resonance
<b>PCA</b>	Principal Component Analysis
<b>PDM</b>	Point Distribution Model
<b>RF</b>	Radio Frequency
<b>RMSE</b>	Root Mean Square Error
<b>SDF</b>	Signed Distance Function
<b>SDM</b>	Signed Distance Map
<b>SSM</b>	Statistical Shape Model
<b>SynN</b>	Symmmetric Normalization
<b>STAPLE</b>	Simultaneous Truth And Performance Level Estimation

**SEGMENTASI HIPOKAMPUS MENGGUNAKAN SET PERINGKAT  
BERASASKAN TERDAHULU BERSEPADU SETEMPAT BERPANDUKAN  
PENDAFTARAN HANYUTAN TITIK KOHEREN TERHIMPUN DAN  
BERWAJARAN**

**ABSTRAK**

Segmentasi hipokampus daripada struktur-struktur subkortikal otak bersebelahan merupakan satu tugas yang sangat mencabar, terutamanya akibat sempadan pemisahan struktur-struktur ini adalah lemah atau kurang jelas, seterusnya menyebabkan pendekatan berasaskan sempadan tidak berkesan untuk segmentasi hipokampus yang betul. Disamping itu, kedudukan hipokampus yang hampir dengan amygdala menyukarkan lagi isu segmentasi. Walau bagaimanapun, trend terkini telah beralih dari bergantung semata-mata kepada ciri-ciri imej kepada penggunaan model-model terdahulu dalam segmentasi. Secara amnya, model-model terdahulu dibina menggunakan segmentasi berasaskan atlas. Walau bagaimanapun, pendekatan ini sangat data intensif kerana ia menggunakan kaedah berasaskan volumetri untuk pembinaan model terdahulu. Oleh yang demikian, tesis ini mencadangkan satu pendekatan pembinaan model terdahulu yang bukan sahaja mampu mewakili maklumat bentuk dan lokasi ruang secara berkesan, malah mempunyai keperluan data intensif yang lebih rendah berbanding pendekatan berasaskan atlas. Secara terperinci, satu kaedah pendaftaran set titik yang novel dicadangkan dan disahkan bagi pembinaan model terdahulu. Pendaftaran set titik yang dicadangkan menggunakan



satu set titik perwakilan dan bukannya keseluruhan isipadu imej dalam membina model terdahulu. Ini membawa kepada sumbangan seterusnya dalam tesis ini, di mana satu set peringkat berasaskan terdahulu bersepadu setempat diperkenalkan bagi segmentasi hipokampus muktamad. Set peringkat berasaskan terdahulu bersepadu setempat ini menggunakan model terdahulu hanya pada lokasi-lokasi yang kekurangan maklumat sempadan bagi menghasilkan segmentasi yang tepat. Ini adalah ciri utama berbanding dengan kaedah-kaedah yang dicadangkan sebelum ini yang melaksanakan integrasi global maklumat terdahulu yang menggunakan model terdahulu pada seluruh domain imej. Penilaian terhadap model terdahulu yang dibina ini telah dijalankan menggunakan set data OASIS-MICCAI. Berbanding pendekatan Bentuk Purata dalam Peta Jarak Bertanda yang lebih terkenal, pendekatan pembinaan model terdahulu yang dicadangkan menunjukkan peningkatan dalam nilai ralat punca purata kuasa dua sebanyak 1.59%, terutamanya bagi menganggarkan hipokampus sasaran yang tidak jatuh dalam populasi latihan. Penilaian juga menunjukkan bahawa pembinaan model terdahulu ini adalah kurang data intensif berbanding pendekatan berasaskan atlas, dari segi bilangan titik data yang digunakan semasa pembinaan. Hasil segmentasi muktamad menunjukkan bahawa prestasi set peringkat berasaskan terdahulu bersepadu setempat yang dicadangkan adalah lebih baik berbanding set peringkat berasaskan terdahulu bersepadu global, dengan peningkatan sebanyak 3.36% dalam nilai pekali persamaan Dice. Perbandingan lanjut dengan pekali persamaan Dice juga telah menunjukkan bahawa hasil segmentasi muktamad adalah setaraf dengan teknik-teknik utama terkini, berprestasi lebih baik berbanding perisian segmentasi hipokampus yang dikenali sebagai Freesurfer. Peningkatan yang menggalakkan yang ditunjukkan oleh kaedah yang dicadangkan dalam tesis ini memberikan satu wawasan

terhadap kegunaan kaedah ini untuk segmentasi hipokampus.

# **HIPPOCAMPUS SEGMENTATION USING LOCALLY INTEGRATED PRIOR-BASED LEVEL SET GUIDED BY ASSEMBLED AND WEIGHTED COHERENT POINT DRIFT REGISTRATION**

## **ABSTRACT**

Hippocampus segmentation from neighbouring brain subcortical structures is a very challenging task mainly because boundaries separating these structures are weak or unclear, rendering conventional edge-based approaches ineffective for proper hippocampus segmentation. Besides that, close proximity of the hippocampus with the amygdala further complicates the segmentation issue. Recent trends, however have shifted from sole reliance on image features to utilization of prior models in the segmentation. Predominantly, the prior models are constructed using atlas-based segmentation. This approach however, is highly data intensive due to the volumetric-based methods used for prior model construction. Consequently, this thesis proposes a prior model construction method that not only effectively represents shape and spatial location information, but also requires lower data intensiveness compared to atlas-based approaches. Specifically, a novel point set registration method is proposed and validated for prior model construction. Instead of using the whole image volume, the proposed point set registration utilizes a set of representative points in constructing the prior model. This leads to the next contribution of this thesis where a locally integrated prior-based level set is introduced for final hippocampus segmentation. The locally integrated prior-based level set used the prior model only at locations with

insufficient boundary information for accurate segmentation. This is the main key feature compared to previously proposed approaches that perform global integration of the prior information, that employed prior model throughout the image domain. Evaluations on the constructed prior model were carried out using the OASIS-MICCAI dataset. Compared to the more popular Mean Shape in Signed Distance Map approach, the proposed prior model construction approach showed improvement by 1.59% in average Root Mean Square Error, especially in generalizing target hippocampus that does not fall within a training population. It is also demonstrated that the prior model construction is less data intensive compared to atlas-based approaches, in terms of number of data points being used during the construction. Final segmentation results indicate that the proposed locally integrated prior-based level set performs better than the globally integrated prior-based level set, with a 3.36% improvement in Dice similarity coefficient value. Further comparisons on Dice similarity coefficient have also shown that the final segmentation results are at par with current state-of-the-art techniques, outperforming a well known hippocampus segmentation software known as Freesurfer. Promising improvement shown by the proposed work in this thesis provide an insight on the applicability of this approach for hippocampus segmentation.

# **CHAPTER 1**

## **INTRODUCTION**

### **1.1 Medical Image Segmentation**

Research into the field of computer aided medical image segmentation has gained much interest in the past decades. This has been motivated by the need for more timely and accurate diagnosis of diseases. Being one of the critical components in medical image processing and analysis, segmentation deals with the identification and delineation of anatomical structure(s) of interest from a stack of medical images. This stack of medical images is also referred to as three dimensional (3D) medical image, or volumetric medical image. The huge proliferation of attention to the segmentation field, as well as the many breakthroughs that have been achieved thus far, demonstrate its relevance and importance to imaging researchers. Despite the considerable successes, effective segmentation remains a very challenging task in producing segmented regions that carry specific visual definitions similar to that of human perception.

Observation of conventional clinical practices shows that medical experts are often able to identify and delineate a target structure accurately based on the perceived image information found explicitly from the medical image combined with the medical knowledge about the structure. This information is illustrated in Figure 1.1. The inherent explicit image information such as the intensity, texture, edge or any second-order or higher-order image features may be procured from the 3D medical

image, specifically via feature extraction techniques (Sonka et al., 1999). Medical knowledge comprises of prior known information about a structure such as the size, shape and its' spatial location in a 3D medical image. Similar to manual expert delineation, a key step in developing a robust automated image segmentation is to enrich the segmentation process with prior information, especially shape and spatial location of the target structure.

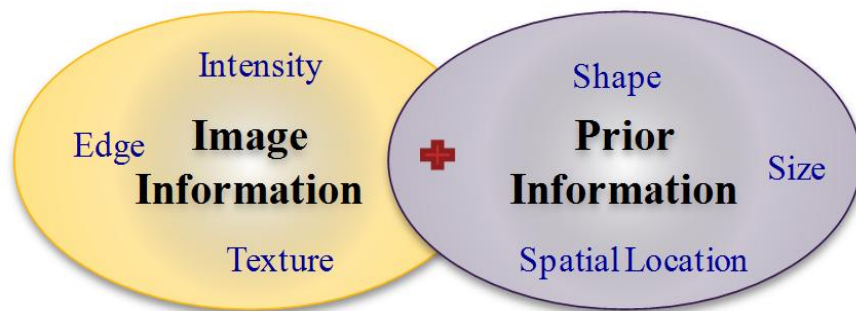


Figure 1.1: Information utilized by medical experts in performing manual delineation.

## 1.2 Trends in Medical Image Segmentation

The evolution in medical image segmentation projected a trend of three eras (Withey and Koles, 2008), as illustrated in Figure 1.2. The first generation started off with conventional segmentation methods that employed only image information. These conventional methods ranged from thresholding (Rosenfeld and Smith, 1981), edge-based (Canny, 1986) and region-based approaches (Chen et al., 2009; Hamarneh and Li, 2009; Ng et al., 2008; Pan and Lu, 2007; Mancas and Gosselin, 2004; Pohle and Toennies, 2001; Yi and Ra, 2001). However, these methods often fail when different structures within an image exhibit almost similar intensity distributions. With closely similar intensity characteristics, a distinctive image feature could not be established to differentiate between the target and neighbouring structures. This has lead to inability

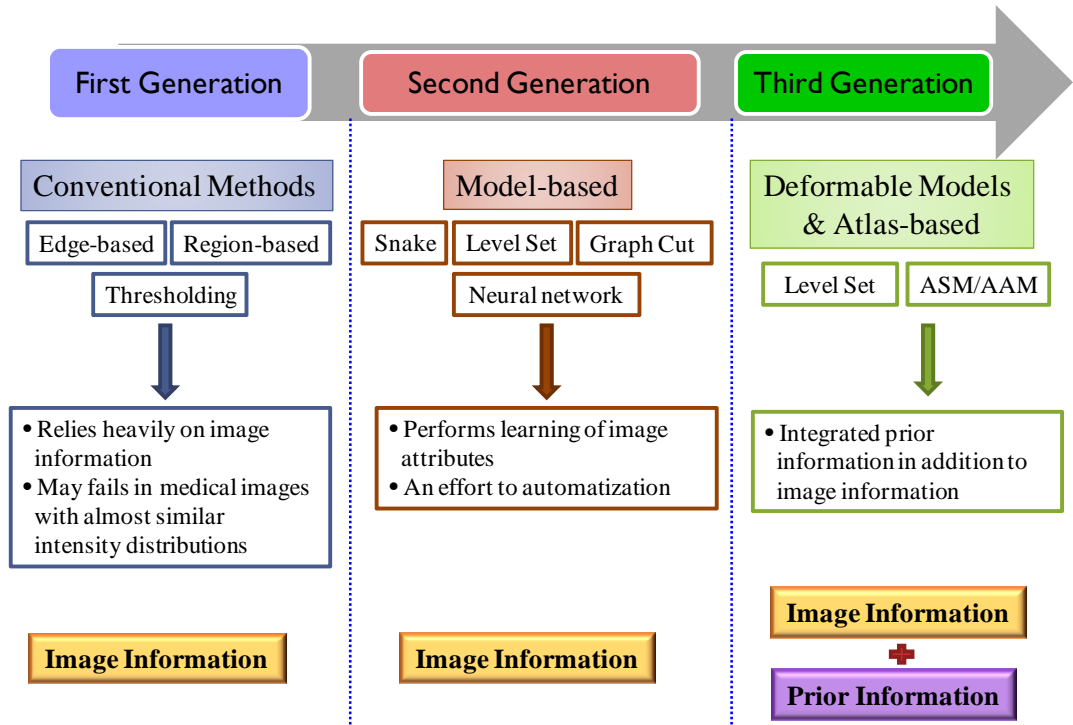


Figure 1.2: The different eras of medical image segmentation.

to produce a complete segmentation.

As an initiative towards automatic segmentation, the second generation of medical image segmentation explored fuzzy and mathematical optimization models to formulate the segmentation problem. These methods use a learning approach to determine a representative set of image features for the target structure. Then, the segmentation finds the target structure having the characteristic of the learned features. Some of the well-established second generation segmentation methods included clustering (Mohamed et al., 1999), classification (Lei and Sewchand, 1992), deformable models (Kass et al., 1988; Osher and Sethian, 1988), graph cuts (Boykov and Jolly, 2000) and neural networks (Cheng et al., 1996). These powerful segmentation methods were able to eliminate heuristic assumption, and lead towards advances in automatic segmentation. However, their robustness was still dependent

upon the image information, which is impractical for segmenting structures with overlapping intensity characteristics such as the brain subcortical structures that exhibits almost identical image features.

Due to the above mentioned shortcomings of the second generation methods, researchers in the third generation of segmentation methods utilized prior information. This generation was perceived to mimic the procedure of medical experts, which integrate image and prior information into the segmentation process. The prior information is usually obtained through a single or a set of training labeled images (manually prelabeled 3D images). Recent developments in inferring prior information during segmentation shows atlas-based segmentation gaining prominence (Landman et al., 2012). The atlas-based approach standardizes a set of training images, and their corresponding training labeled images into a standard space and uses label fusion to assemble the standardized training labeled images to produce the final segmentation.

Another category of well known segmentation methods known as deformable models have also demonstrated the incorporation of prior information to assist segmentation. These deformable models cover Active Shape Model (ASM) (Cootes et al., 1995), Active Appearance Model (AAM) (Cootes et al., 2001), snake and level set methods (Rousson and Paragios, 2002). These deformable models use prior information in the form of a set of shape variations learned from a training population. The deformable models then, iteratively deform in an energy minimization framework to deform an initial model towards a target structure, constraining the deformation to be within the specified shape variations.



From the medical image segmentation literature, integration of prior information with image information is the *de-facto* standard of current medical segmentation methods. This integration takes advantage of the idea in clinical manual delineation that uses the prior information, with the aim of accomplishing a more accurate segmentation.

### 1.3 Hippocampus

The word **Hippocampus**, meaning *Seahorse* in Latin, was adapted to refer to the brain hippocampus due to its similar appearance to the shape of a seahorse. The hippocampus is a pair of mirrored structures found on the left and right hemisphere of the brain. They are very small subcortical structures (structure beneath the cerebral cortex) located inside the medial temporal lobe (Duvernoy, 2005). Figure 1.3 illustrates the location of the hippocampus in reference to the temporal lobe. The curved shaped hippocampus is divided into three major parts, which are the head, body and tail. The head appears to be larger compared to its narrower tail (as shown in Figure 1.4). The amygdala is the most closely located subcortical structure at the head of the hippocampus. Figure 1.5 provides an example of brain Magnetic Resonance (MR) image, with the hippocampus being highlighted in axial, coronal and sagittal views.

Associations between the hippocampus with human memory and emotion have led to a multitude of clinical studies relating to diseases such as Alzheimer's, mild cognitive impairment, schizophrenia, and epilepsy (Mumoli et al., 2013; Maller et al., 2012; Salmah et al., 2011; Shi et al., 2009; Gerardin et al., 2009). In these clinical

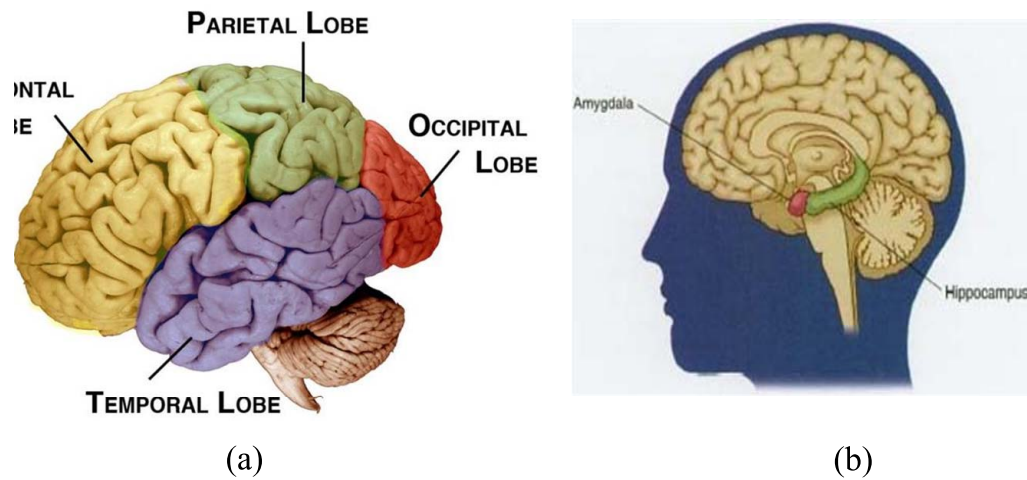


Figure 1.3: (a) Anatomy of the brain, relating to the location of temporal lobe (*Serendip Studio*, 2015). (b) The location of hippocampus in the brain (*Human Illnesses and Behavioral Health*, 2015).

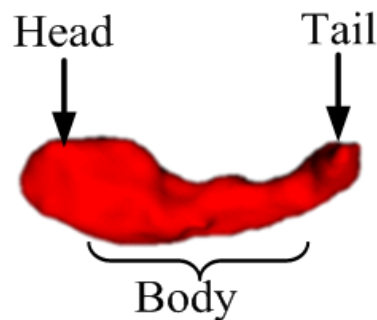


Figure 1.4: Overview of the hippocampus structure (*IcoMetrix*, 2015).

studies, researchers focus on establishing a correspondence between the hippocampus volume and shape of normal subjects and subjects with pathological disorders. Most of these researchers are still dependent on manual delineation on every two dimensional (2D) image slices before the analysis of volume and shape can be performed.

Manual delineation is an intensive procedure, time consuming and difficult to perform. In addition, it is also often associated with interrater and intrarater variability,

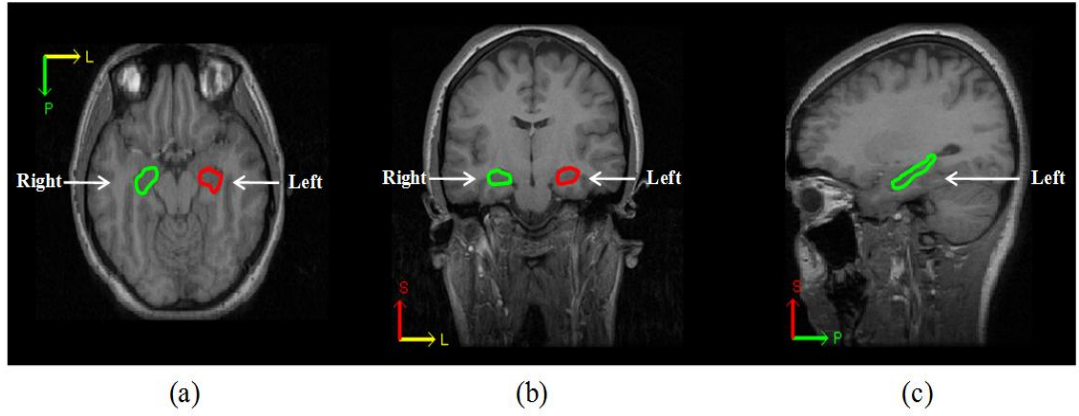


Figure 1.5: Hippocampus being highlighted in green (right hippocampus) and red (left hippocampus) in (a) axial, (b) coronal, and (c) sagittal views, respectively.

which may lead to the issue of reliability of the delineated hippocampus. Therefore, the need for automated segmentation solutions arises as a precondition for accurate and efficient morphometric analysis of the hippocampus. This can hence better illustrate the relationship between the hippocampus and brain-related disorders (Nestor et al., 2013; Lotjonen et al., 2011).

#### 1.4 Problem Statement

Segmentation of the subcortical structures in the brain such as the hippocampus, is known to be very challenging owing to its' image characteristics. In brain MR images, the hippocampus is observed as a gray matter structure that often times, exhibit very weak or unclear boundary definitions at some fragments of its' boundary. This happens due to almost similar or overlapping intensity distribution between hippocampus and other adjacent gray matter structures, such as the amygdala (Manjon et al., 2007). Besides that, close proximity of the hippocampus with the amygdala further complicates the segmentation issues (Boccardi et al., 2011; Sanchez-Benavides et al., 2010; Morey et al., 2009). The close proximity between the hippocampus and

the amygdala is shown in Figure 1.6.

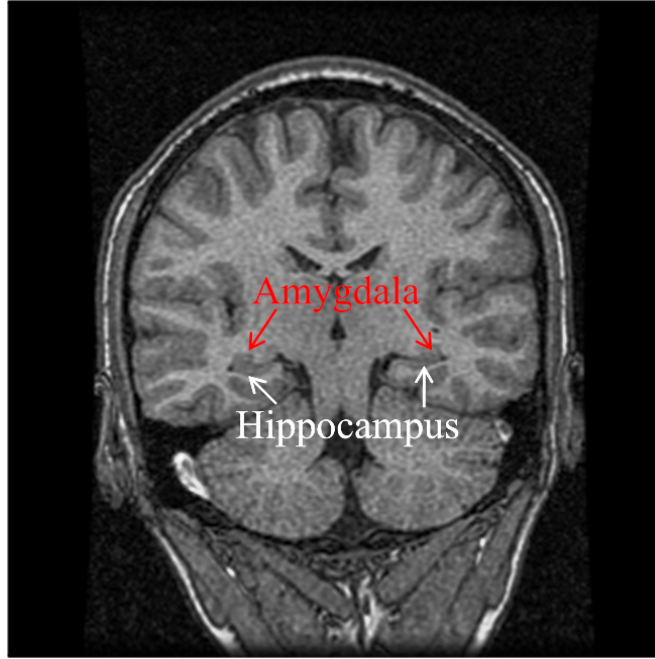


Figure 1.6: An example of a brain MR image in the coronal view, highlighting the hippocampus and the amygdala.

Generally, poorly visible hippocampus boundary has become a major deterrent for effective segmentation. Even the medical experts tend to misjudge the hippocampus boundary due to this problem, especially at the head and tail. A poorly defined boundary usually causes the ambiguity on the exact location representing the hippocampus boundary. With these main challenges being demonstrated by hippocampus, relying on image information alone may not produce the desirable segmentation results. Therefore, prior information such as shape and spatial location need to be incorporated into existing segmentation methods to improve the segmentation results. The *shape information* reflects the 3D geometric shape that may be seen visually, and the *spatial information* should denote the spatial coordinate space that a target structure occupies within an image.

To propose a method that can effectively incorporate prior information for hippocampus segmentation, the following questions need to be answered:

**(i) *How to automatically construct a model representing the required prior information, that consists of both shape and spatial information?***

There are two main sources for obtaining prior information of brain structures:

(i) Standard public atlases. (ii) Training dataset comprising of labeled images.

Among the two, a training dataset seems to be more suitable because it can reflect the target image better, which is acquired with similar image acquisition protocols. Currently, enormous research interest has focused on constructing prior information from the training dataset, which in the literature is referred to as *atlas or model construction* (Landman et al., 2012). The constructed atlas or model is the statistical representation of prior information. The atlas-based approaches are used to construct an atlas. The constructed atlas is a voxel-based statistical model. This atlas gives the spatial distribution of probability for every voxel belonging to a target structure (Cabezas et al., 2011). This atlas provides the shape and spatial information. However, due to the use of 3D volumetric labeled image during atlas construction, the atlas-based approaches are known to face high data intensiveness. In the context of this thesis, this *data intensiveness* refers to the number of data points (i.e. voxels as for 3D image) being used during the construction of the final atlas or model. Another form of prior information is given by the Statistical Shape Model (SSM), which can be built using only landmark points on the surface of a structure (Heimann and Meinzer, 2009). This SSM is mostly interested in constructing the mean shape and a range of shape variations within a training population. Thus, SSM are usually computed

in a coordinate space of a chosen reference image, and not on the coordinate space of the target image. This causes the SSM to contain only the spatial information of the reference image space, and not the actual target image space. Hence, the SSM exhibits less accurate spatial information of a target structure. A prior model would be most beneficial for segmentation if it contains both, shape and spatial information. Besides that, the process of constructing the prior information should also be less data intensive and automated.

**(ii) *How prior information is of assistance in segmentation?***

It has been established in Section 1.1 that prior information is essential for assisting the segmentation process. Therefore, the chosen segmentation method must be able to utilize both image and prior information during segmentation. By taking both criteria into consideration, it appears that the level set method may be suitable for segmenting the hippocampus. Level set method allows the integration of various types of image and anatomical features within a single energy minimization framework. Each desired feature of a target structure can be modeled as an energy term and incorporated into the level set evolution function (Chan and Zhu, 2005; Vese and Chan, 2002). However, two main issues exist in using level set for hippocampus segmentation. These issues are the requirement of (i) proper initialization, and (ii) a stopping force for the evolving level set. Incorrect initialization placed far away from or outside of the hippocampus may lead the level set to be directed to segment other irrelevant neighbouring structures, such as the amygdala which are located very closely to hippocampus. Therefore, placement of initialization inside the hippocampus region is very crucial in ensuring accurate segmentation. The hippocampus is also

known to consists of fragments of strong, weak and missing boundary definitions. The weak or missing boundaries happen especially at the head and tail portions. A reliable stopping force is therefore imperative in order to stop the evolving level set at these boundary fragments, so that leaking into adjacent structures is avoided. In conventional manual delineation, experts refer to the image features to identify the hippocampus. Whenever a clear distinction between image features could not be established, then only the prior information involving approximate spatial location and shape of the structure is used. Therefore, a robust hippocampus segmentation method should not be fully dependent upon prior information. The prior information should only be an assistance for the segmentation in cases where the image features is not sufficient or missing at certain fragment of the hippocampus boundary. The manner of utilizing either image or prior information only at a particular fragment or portions in an image is defined to be *locally* inferred image or prior information. This scenario is illustrated in Figure 1.7, which shows a synthetic image with weak or missing edge information at some part of its boundary. In such cases, prior information of the object is only needed locally at the weak or missing edge fragments, whereas, at the edge with strong edge information, the edge gradient may be useful.

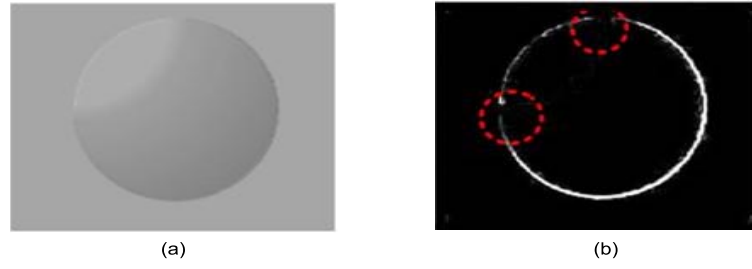


Figure 1.7: (a) A sample of synthetic image. (b) Edge gradient magnitude of the synthetic image with the weak or missing edges highlighted.

## 1.5 Objectives

The major aim of this research is to propose a segmentation approach that is able to utilize prior information locally to segment the hippocampus from brain MR images.

This work attempts to achieve the main objective through the following:

- (i) To automatically construct a prior model, which is able to exhibit shape and spatial information of the hippocampus with less data intensiveness.
- (ii) To propose a 3D level set method, integrating prior information locally to segment the hippocampus.

## 1.6 Scope

The scope of this thesis is limited to certain constraints, which are defined as follows:

- T1-weighted MR image is the preferred modality to view or delineate brain anatomical structures. Hence, this study is limited to study T1-weighted brain MR images.
- The dataset being used in this work only comprises of normal hippocampus



studies without any pathological issues. This is because subjects with pathological disorders may exhibit abnormal hippocampus shapes and sizes, which is not the focus of this thesis.

### **1.7 Significance of the Study**

The main significance of this research is its profound implications in clinical practice. Traditionally, many standard protocols exist in clinical practice to ease the manual delineation process. However, this process is still laborious and time consuming. The proposed automated segmentation approach in this thesis will be able to facilitate timely hippocampus morphometric analysis in clinical studies.

### **1.8 Overview of Methodology**

The methodology applied in this thesis consists of two main phases. The first phase involves the construction of prior model of hippocampus. This prior model shall consists of both, shape and spatial information. In this phase, a new point set registration approach that produces the prior model of hippocampus is proposed. This phase is described in detail in Chapter 5.

The second phase proposes a level set method, assisted by the prior model constructed in the first phase to segment the hippocampus. The prior model is used to provide 3D initialization to the level set. In addition, the prior model is also formulated as a stopping force in the level set method to prevent leakages into adjacent structures, where the image features are unable to provide sufficient boundary definition. The main contribution of the second phase is the integration of image and prior information

in a local manner. The details pertaining to the proposed segmentation approach is described in Chapter 6. Evaluations on the proposed phases are verified using two widely known public brain datasets.

## **1.9 Contributions**

This thesis has led to four main contributions, which are detailed as follows:

1. Establishing a new method to automatically construct the prior model of hippocampus. The established method provides an alternative way of constructing the prior model, against the widely used atlas-based approaches. The proposed method is also less data intensive. Experimental results show that the constructed prior model is able to provide shape and spatial information of a target hippocampus.
2. Providing a new approach to enable automatic initialization for a 3D level set using the constructed prior model. The automatic initialization inside the hippocampus is very crucial because hippocampus is a very small structure, and closely adjacent to other gray matter structure. Thus, it is very important to initialize the level set inside the target hippocampus.
3. Proposing a new level set method that integrates prior information with image information in a local manner. This locally integrated prior-based level set is able to prevent leakages commonly faced in conventional level set methods, and segment the hippocampus. Besides that, the proposed locally integrated prior-based level set is also able to perform comparably better than globally integrated prior-based level set.

4. Proposing a full pipeline for hippocampus segmentation. The comparison with state-of-the-art hippocampus segmentation approaches has shown that the proposed segmentation approach is at par with the state-of-the-art. This comparison validates the main objective of this thesis, which is the segmentation of the hippocampus.

## **1.10 Organization of the Thesis**

This thesis is organized into seven chapters as follows:

**Chapter 1** introduced the trends and issues in medical image segmentation. In addition, this chapter provided an insight to hippocampus segmentation issues that will be addressed in this thesis. Discussions on the objectives, scope, and contributions have also been highlighted accordingly.

**Chapter 2** presents the fundamental concepts relevant to the work in this thesis. This chapter serves as the foundation for brain Magnetic Resonance Imaging modalities, medical image registration and level set methods.

**Chapter 3** provides a critical review of state-of-the-art methods in brain structures segmentation and prior-based level set methods.

**Chapter 4** delivers an overview of the methodology adapted in this thesis for segmenting the hippocampus. This chapter also covers detailed information on the brain datasets and evaluation measures used in this research.

**Chapter 5** presents the first phase of this research, which is the Prior Model

Construction. This phase constructs the prior model of the hippocampus. This chapters covers detailed explanations on the proposed approach and is validated with supporting experimental results.

**Chapter 6** describes the second phase of this research on how the constructed prior model is utilized to infer the initialization and stopping force for the level set method. The proposed locally integrated prior-based level set is explained in detail. Comparisons with state of the art segmentation approaches are also presented to highlight the performance of the proposed segmentation approach.

**Chapter 7** offers a summary of this research, and draws conclusions from the results. A perspective into future direction coming out of this research is also presented.

## **CHAPTER 2**

# **BACKGROUND**

This chapter presents the fundamental background that are relevant to this research. Section 2.1 firstly introduces Magnetic Resonance Imaging and its application in acquiring the brain anatomy. Section 2.2 then proceeds to the topic of medical image registration. Finally, Section 2.3 briefly gives an overview of deformable models segmentation, focusing on important definitions and mathematical models of level set.

### **2.1 Magnetic Resonance Imaging**

Magnetic Resonance Imaging (MRI) is a noninvasive imaging technique used to produce high quality mapping of internal anatomy and functions inside the body (Adam and Dixon, 2008). Since its introduction in 1970s, MRI has revolutionized the field of diagnostic medicine. MRI uses very low energy and non-ionizing electromagnetic radiation, which frees subjects from harmful exposure (Adam and Dixon, 2008). MRI basically absorbs and emits Radio Frequency (RF) waves with magnetic field occurrences to form cross-sectional images of the body. The Magnetic Resonance (MR) images are constructed based on the concept of capturing the Nuclear Magnetic Resonance (NMR) signal of molecules in the human body. The human body is primarily composed of water and fat, with hydrogen being its main molecule. The emitted RF waves are absorbed by the hydrogen molecule, which causes the molecules to move. These movements emit energy, which is captured as NMR signals by the MRI

machine. Eventually, the captured signals are processed and generated as a 3D image or volumetric image. Different tissues possess varying levels of hydrogen. Therefore, the emitted energy also varies depending on the body tissue type. This results the captured signals to project varying strength of 3D image feature, denoted by the image intensity.

### **2.1.1 Imaging Characteristics**

The main advantage of MRI is its ability to produce high resolution imaging of soft tissue (Hornak, 2014). In addition, it allows tailoring of multiple contrast of image in accordance to the case of study. Generally, the contrast variables are created by varying the pulse sequences and imaging parameters. The pulse sequences comprises of Proton Density (PD), spin-lattice relaxation time (T1), and spin-spin relaxation time (T2). The imaging parameters on the other hand consist of repetition time, echo time, inversion time and rotation angle. Readers can be directed to Adam and Dixon (2008) for more detailed and technical explanations regarding the contrast parameter settings. In MRI, an image data is referred according to the pulse sequences being utilized, i.e. *T1-weighted MR image* denoting image captured using contrast based predominantly on the T1 pulse sequence.

### **2.1.2 Imaging Coordinates and Planes**

The 3D spatial coordinates in MRI is commonly referred to as the *anatomical coordinate system* (Hornak, 2014). Figure 2.1 illustrates the imaging coordinates and planes in MRI.

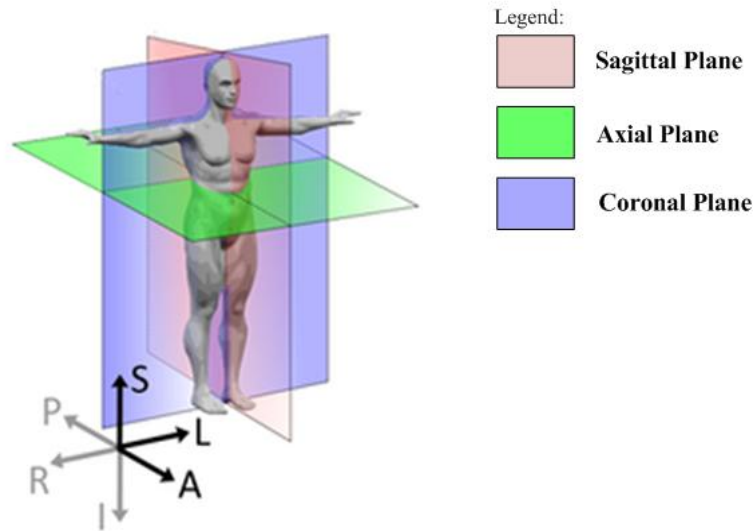


Figure 2.1: The imaging coordinates and planes in MRI (*3D Slicer*, 2015).

This system references the body according to three axes which are:

- (a) Left-Right (L-R)
- (b) Superior-Inferior (S-I)
- (c) Anterior-Posterior (A-P)

The anatomical coordinate system describes an anatomical position based on the three planes that are perpendicular to the L-R, S-I and A-P axes. These planes are termed as:

- (a) **Sagittal** plane that bisects the left and right side of the body.
- (b) **Axial** plane that is perpendicular to the S-I axes, separating the upper (S) and lower (I) part of the body.
- (c) **Coronal** plane that separates the front (A) from the back (P) of the body.

An anatomical position in a MR image is referred to as a voxel (x,y,z coordinates in the 3D space) if it is a volumetric image, or pixel (x,y coordinates in the 2D Euclidean space) if it is only an image from the respective plane.

### **2.1.3 Brain Magnetic Resonance Imaging**

The brain is a collective formation of soft tissues, which appears to be almost similar in appearance. Hence, the capability of MRI at capturing small intensity variations between tissues and producing it as high contrast imaging of soft tissues seems to be very advantageous for brain imaging. The growing demand for brain MRI in clinical applications proves that it is the state-of-the-art of current brain imaging technology (van der Kolk et al., 2013). Brain MRI is primarily used to analyze the structure and functionality of the human brain, which may assist in early detection of abnormalities and disease progression (Schmidt et al., 2011; Nanjundaswamy et al., 2011; Jack et al., 2008).

Clinical diagnosis is also made easier with the ability to visualize variety of imaging contrasts during a single scanning procedure. This allows medical experts to make more accurate clinical diagnosis based on complementing information from multiple contrast modalities. As an example, Figure 2.2 compares a T1-weighted and T2-weighted brain MR images. Here, the brain tumour appears to be more apparent in the T2-weighted MR image, whereas it looks almost similar to normal tissue in the T1-weighted MR image. Thus, having multiple contrasting images allows better decision making by the medical experts.



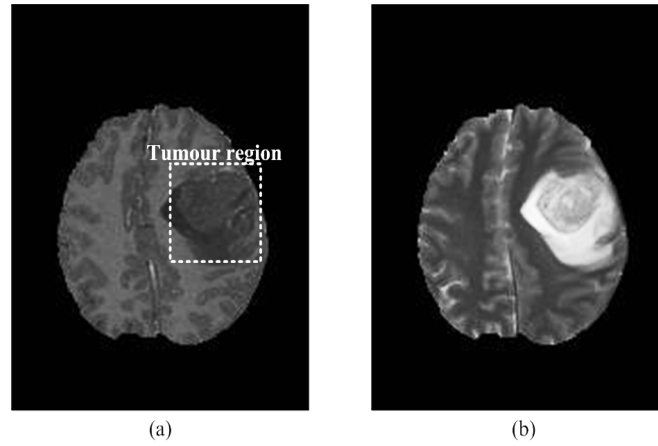


Figure 2.2: Comparison between (a) T1-weighted and (b) T2-weighted brain MR images (*BRATS: Multimodal Brain Tumor Segmentation Challenge*, 2015).

## 2.2 Medical Image Registration

Medical images are susceptible to intersubject, intermodality, intertemporal (images of the same subject taken at different time frames) and intersequence (images of an anatomy taken for a sequence of time step) variability. In clinical decision making, these images are very useful to be exploited for the information that may be gained from plethora of high resolution images. However, fair comparisons between multiple medical images may only be performed if all the images are within a common standard space, and without any variations contributed due to the image acquisition process. One solution to tackle such invariability among images is through *medical image registration*. Image registration can be seen as a preprocessing stage, where all medical images are standardized to be within a common standard space.

Medical image registration aligns a set of images into a standard space through an optimal geometric transformation (Maintz and Viergever, 1998). This transformation is found by maximizing or minimizing a similarity cost function, formulated based on a similarity measure defined using either statistical or geometrical features of

the images. Classification of the enormous number of registration approaches that have been proposed may follow different perspectives, and have led to several survey papers focusing on these groupings (Oliveira and Tavares, 2014; Makela et al., 2002; Maintz and Viergever, 1998). In this section, the registration approaches are discussed based on two major viewpoints: (i) The type of transformation, and (ii) The nature of registration algorithms. The following sections detail these two viewpoints accordingly.

### 2.2.1 Type of Transformation

The commonly practiced transformation paradigms in medical image registration, especially in brain imaging are *rigid*, *affine* and *non-rigid* transformations. *Rigid* transformation allows only rotations and translations in aligning the images, where it maintains the original shape and size of the target object. It is defined by six transformation parameters, or degrees-of-freedom, comprising of three parameters for rotation and three parameters for translation (Oliveira and Tavares, 2014). An extension to rigid transformation that includes additional scaling and shearing is referred to as *affine* transformation (Jenkinson and Smith, 2001). Rigid and affine transformations are commonly treated as preprocessing procedures in aligning whole brain images into a common coordinate system and principal axes (Ashburner and Friston, 2004).

*Non-rigid* transformation allows local transformation or deformation by using additional transformation parameters of local free form deformations (Crum et al., 2004). Due to this local transformation, the original shape of the target object is

usually deformed according to the transformation parameters being applied. Generally, non-rigid transformation is applied in the literature to analyze changes or motion of anatomical structures over a time (Carbayo et al., 2006; Tom et al., 1994), and to standardize intersubject correspondences for model or atlas construction (Cabezas et al., 2011; Cootes et al., 2010, 2004; Joshi et al., 2004; Collins et al., 1994).

### **2.2.2 Nature of Registration Algorithms**

Review on registration algorithms show that medical image registration can be divided into two main algorithmic categories, namely *global* and *local* (Oliveira and Tavares, 2014). *Global* registration, which is also known as volumetric registration, uses the whole dataset (all voxels) in finding the correspondences during the transformation. The global registration usually utilizes intensity or voxel's statistical features in matching the correspondences between two medical images (Reducindo et al., 2013; Andersson et al., 2007; Rueckert et al., 1999; Collins et al., 1994).

On the contrary, the *local* registration only selects a subset of voxels in finding the correspondences during the transformation (Hajnal et al., 2001). This subset may comprises of fiducial markers or landmark points (Li and Kurihara, 2014; Chui and Rangarajan, 2003; Hartkens et al., 2002; Rohr et al., 2001; Thirion, 1996), contour or surfaces (Anticevic et al., 2012; Pantazis et al., 2010; Subsol et al., 1997), or subvolumes (Riklin-Raviv et al., 2010; Ourselin et al., 2000).

## 2.3 Deformable Models

Deformable models have been extensively researched and successfully applied for the segmentation of anatomical structures. The deformable models allow the integration of image and prior anatomical information through an optimization framework, which enables any types of desired segmentation to be designed. This grants formulation of the deformable models to be specifically tailored for the problem at hand.

Deformable models are curves (2D), surfaces or hypersurfaces (3D) defined within an image domain, under the influence of *external* and *internal* energies (Xu et al., 2000). The deformable models evolve based on the driving forces defined by the external energy represented by image features such as edges or intensity towards the target object, while retaining the shape and smoothness of the model (internal energy). The idea of deformable model is pioneered in the 1970s by Widrow (1973)'s rubber mask technique and Fischler and Elschlager (1973)'s spring-loaded templates for modeling and representing objects. However, the deformable models only became prominent after its introduction into the field of computer vision and graphics by the seminal work of Terzopoulos et al. (1988). In the literature, the main techniques of deformable models fall under two main categories, which are *parametric* and *level set*. The following describes these methods detailing the important concepts and characteristics.

### 2.3.1 Parametric Models

Parametric model evolves a curve or surface explicitly through displacement of a set of control points on the curve or surface from an initial position. These control points